Metabolic Engineering 14 (2012) 661–671

Contents lists available at SciVerse ScienceDirect

Metabolic Engineering

journal homepage: www.elsevier.com/locate/ymben

A dynamic metabolite valve for the control of central carbon metabolism

Kevin V. Solomon [a], Tarielle M. Sanders [a,b], Kristala L.J. Prather [a,*]

[a] Department of Chemical Engineering, Synthetic Biology Engineering Research Center (SynBERC), Massachusetts Institute of Technology, Cambridge, MA 02139, USA
[b] Amgen Scholars Program, Department of Chemistry, Norfolk State University, Norfolk, VA 23504, USA

ARTICLE INFO

Article history:
Received 12 August 2012
Received in revised form
22 August 2012
Accepted 26 August 2012
Available online 28 September 2012

Keywords:
Glucose utilization
Flux optimization
Growth mediated buffering
Inverters
Synthetic biology

ABSTRACT

Successful redirection of endogenous resources into heterologous pathways is a central tenet in the creation of efficient microbial cell factories. This redirection, however, may come at a price of poor biomass accumulation, reduced cofactor regeneration and low recombinant enzyme expression. In this study, we propose a metabolite valve to mitigate these issues by dynamically tuning endogenous processes to balance the demands of cell health and pathway efficiency. A control node of glucose utilization, glucokinase (Glk), was exogenously manipulated through either engineered antisense RNA or an inverting gene circuit. Using these techniques, we were able to directly control glycolytic flux, reducing the specific growth rate of engineered *Escherichia coli* by up to 50% without altering final biomass accumulation. This modulation was accompanied by successful redirection of glucose into a model pathway leading to an increase in the pathway yield and reduced carbon waste to acetate. This work represents one of the first examples of the dynamic redirection of glucose away from central carbon metabolism and enables the creation of novel, efficient intracellular pathways with glucose used directly as a substrate.

1. Introduction

Microbes are powerful manufacturing platforms for a wide array of chemicals and compounds from renewable resources (Curran and Alper, 2012). Optimization of these processes for economic viability, however, remains a significant challenge. In addition to potential issues with catalytic activity, engineered pathways frequently compete with endogenous ones for common substrates. To address this issue, metabolic engineers typically knock out the competing pathways or overexpress the production pathway enzymes to drive the flux towards the target compound. However, for pathways that compete with essential and/or catalytically efficient processes, these approaches are not necessarily feasible and call for tunable control of the competing pathway. Recent works by ourselves and others (Asadollahi et al., 2008, 2010; Becker et al., 2010, 2009; Biedendieck et al., 2009; Kim et al., 2009; Solomon et al., 2012) have demonstrated that tuning expression of these endogenous competing enzymes is a viable method of improving the yield and/or titers of desired heterologous pathways. When glycolysis itself is the competing pathway, however, unique challenges arise.

Central carbon metabolism is tightly regulated and controls processes integral to cell growth and proliferation. Thus, the tuning of carbon flux through central metabolism yields pleiotropic effects. These include obvious phenotypic effects such as changes in biomass accumulation (Cho et al., 2012) and specific growth rate (Callura et al., 2012; Solomon et al., 2012) as well as more subtle and far ranging global consequences of protein expression (Klumpp et al., 2009; Scott et al., 2010). When placed in the context of heterologous production, these changes may have an unforeseen impact on the ability of the cell to express the necessary recombinant genes or maintain cofactors at optimal levels (Heyland et al., 2011; Solomon et al., 2012). For all these reasons, a dynamic tuning system to control central carbon metabolism, which we call a *metabolite valve*, is needed. With a valve, one could potentially maximize heterologous productivity by optimizing pathway efficiency, recombinant protein expression, and biomass and intracellular resources accumulation with timed manipulations of central metabolism.

To fully realize the potential of dynamic control in such systems, one need only consider the natural example of secondary metabolism (Demain, 2000; Drew and Demain, 1977). Secondary metabolites display the interesting property of being preferentially accumulated once growth has ceased. This separation in growth and production, however, allows for dramatic secondary metabolite overproduction as their primary metabolite precursors are no longer required for growth. Similarly, a dynamic valve would allow one to artificially induce secondary metabolism; cultures would accumulate biomass at

* Correspondence to: Department of Chemical Engineering, 77 Massachusetts Avenue, Room 66-454, Cambridge, MA 02139, USA. Fax: +1 617 258 5042.
E-mail address: kljp@mit.edu (K.L.J. Prather).

1096-7176/$ - see front matter © 2012 Elsevier Inc. All rights reserved.
http://dx.doi.org/10.1016/j.ymben.2012.08.006

wildtype rates and once a target cell density is achieved, the system would downregulate endogenous metabolism, redirecting flux of carbon away from growth into product formation. In such environments, the traditional paradigm of an inducible promoter to trigger an OFF to ON state for gene expression is no longer feasible; such systems would necessitate a costly separation process to remove the inducer in the shift from biomass to product formation. Similarly, while repressible promoter systems do exist, they are less well characterized for metabolic engineering applications and are tied to the regulation of endogenous processes, limiting the ability to achieve orthogonal control of the system (Lim et al., 1987; Shimizu et al., 1973; Shoeman et al., 1985; Stojiljkovic et al., 1994). Thus, we explored the potential of orthogonal, engineered systems with the desired inverse input–output relationship, namely, inducible antisense RNA and an inverting gene circuit (inverter). Such systems have enjoyed a number of successes in diverse applications ranging from the control of bioprocesses (Desai and Papoutsakis, 1999; Kim et al., 2009; Kim and Cha, 2003; Tummala et al., 2003a, 2003b) to the design of complex devices (Callura et al., 2012; Isaacs et al., 2004; Tabor et al., 2009; Yokobayashi et al., 2002).

We recently demonstrated the ability to control carbon flux in a PTS$^-$ Glu$^+$ mutant of *Escherichia coli* through control of glucokinase (Glk) activity (Solomon et al., 2012). While the system was able to control the yield of a model glucose consuming pathway, this control was static. Moreover, due to the lack of alternate routes of carbon utilization, the permanent changes in Glk expression had negative effects on the ability of the cell to express recombinant enzyme and simultaneously support growth. In this study, we explore dynamic control of Glk and its impact on heterologous pathway productivity. Through antisense RNA and inverters, we were able to inhibit Glk activity by up to 25% and 50% respectively. Furthermore, through dynamic control with the inverter, we were able to observe improvements in titers and yields of a model compound, gluconate, and decrease in carbon waste to acetate, not only as a function of induction, but also timing of induction. These improvements were not accompanied by the limitations seen in the static system. This work provides further evidence of the feasibility and impact of the control of glycolysis through Glk as well as illustrates a few advantages and challenges of dynamic control.

2. Materials and methods

2.1. Strains and plasmids

E. coli strains and plasmids used in this study are listed in Table 1. All molecular biology manipulations were carried out according to standard practices (Sambrook and Russell, 2001). Molecular cloning and vector propagation were performed in *E. coli* DH10B (*F$^-$ mcrA* Δ(*mrr-hsdRMS-mcrBC*) *φ*80*lacZ*Δ*M*15 Δ*lacX*74 *recA*1 *endA*1 *araD*139 Δ(*ara, leu*)7697 *galU galK λ$^-$ rpsL nupG*) (Invitrogen/Life Technologies, Carlsbad, CA). Antisense control of glycolytic flux was tested in the previously constructed PTS$^-$ Glu$^+$mutant KTS622 (Solomon et al., 2012). Gluconate production in strains bearing multiple plasmids was tested in KTS022IG, KTS622IG, KTS822IG and KTS922IG of the glucokinase expression family (Solomon et al., 2012). Glucokinase expression was controlled by replacing the native primary promoter of *glk* with a constitutive promoter from the Anderson promoter library (http://partsregistry.org). A medium-copy tet-inducible vector for antisense induction was created by PCR amplifying the pBAD30 backbone (Guzman et al., 1995; ATCC, Manassas, VA) and TetR cassette of pWW308 (Moon et al., 2010; provided by John Dueber, UC Berkeley), and ligating them together at introduced AvrII and XhoI sites. Antisense constructs were amplified with HotStarTaq (Qiagen, Valencia, CA) from DH10B genomic DNA and cloned into pBAD30 using the introduced SalI and EcoRI cloning sites. These constructs were later subcloned into pKVS45 using the same sites. Subsequent sequencing revealed the constructs had more than 99% complementarity with the target mRNA except a single point mutation in all but R756. These point mutations were unique to each construct. Gdh was subcloned from pTrc99 Cm-Gdh (Solomon et al., 2012) into pBAD30 using XbaI and HindIII restriction sites. Unless otherwise noted, PCR amplifications were performed with Phusion High-Fidelity DNA Polymerase (NEB, Ipswich, MA) and oligonucleotides from Sigma-Genosys (St. Louis, MO; Table 2). Restriction enzymes and T4 ligase were also obtained from NEB.

2.2. Inverter construction

tetR and *lacI* cassettes as described in Section 3.3 were synthesized by GenScript (Piscataway, NJ). The *tetR* cassette comprised the region spanning bases 5′-GTCGACTCGACTCTAGTGG through the XhoI site inclusive of pKVS45 with J61048, a transcriptional terminator from the Registry of Standard Biological Parts (http://partsregistry.org), fused directly to the 3′ end. The *lacI* cassette consisted of P_{tet} from pKVS45 (bases spanning 5′-CTAAGAAACCATTATT through 5′-ATACTGAGCACCTAGGT inclusive) directly fused to B0034, a ribosome binding site, *lacI-LVA* (C0012) and B0015, a transcriptional terminator, all from the Registry. To facilitate modular inverter designs, the *tetR* and *lacI* cassettes were then amplified with the primers indicated in Table 2 and assembled with standard cloning techniques. This strategy allowed us to directly incorporate the promoters used to drive *glk* expression and the *lacO* operator site into the primers for *lacI* amplification. The final designs were generated without the terminator B0015 and used either the promoter J23114 or J23117 (http://partsregistry.org) for expression of *glk* as discussed in Section 3.3. Assembled constructs were cloned into the plasmid pTKIP-neo (Kuhlman and Cox, 2010).

Final constructs were integrated into the genome of KTS022IG, a mutant that cannot metabolize gluconate (Solomon et al., 2012), directly upstream of *glk*, replacing the FruR binding site through the primary promoter using the method of Kuhlman and Cox and helper plasmids pTKRED, pTKS/CS and pCP20 (Kuhlman and Cox, 2010). Briefly, a TetA landing pad, amplified from pTKS/CS, was integrated into the 5'UTR of *glk* in KTS022IG with pTKRED. Successful integrants were selected on tetracycline and verified by colony PCR. pTKIP-neo plasmids containing the completed inverters (pTKIP-neo-KI06 and pTKIP-neo-KI09) were then used to transform KTS022IG bearing the landing pad and pTKRED. Homing endonuclease, I-SceI, and λ-Red recombinases were expressed from pTKRED to integrate the completed inverter. The integrated design was selected on kanamycin. FLP recombinase expressed from pCP20 (Datsenko and Wanner, 2000) was used to cure the *neo* marker. Finally, all helper plasmids were cured from the final constructs of NVS622IG and NVS922IG. All mutants were identified and isolated by colony PCR with appropriate primers. The final integrated constructs were further verified with sequencing of colony PCR products.

2.3. Culture conditions

Strains were propagated in Luria–Bertani (LB) medium at 37 °C for daily manipulations (30 °C for intermediate recombination steps). Temperature sensitive plasmids were cured at 42 °C on non-selective medium. All experimental cultures were grown at 37 °C in M9 minimal medium supplemented with 0.8 mM L-leucine and either glucose or glcycerol as indicated. For all experiments, seed cultures were grown to an OD measured at a wavelength of 600 nm (OD_{600}) of at least 0.2 before being transferred to a 50 ml culture of the same medium. For experiments involving pTrc99

Table 1
Strains and plasmids.

Name	Relevant genotype	Source
***E. coli* strains**		
Electromax DH10B	*F⁻ mcrA Δ(mrr-hsdRMS-mcrBC) φ80lacZΔM15 ΔlacX74 recA1 endA1 araD139 Δ(ara, leu)7697 galU galK λ⁻ rpsL nupG*	Invitrogen
KTS022	DH10B *ΔptsHIcrr galP^q*	(Solomon et al., 2012)
KTS622	KTS022 P_{glk}::*J23117*	(Solomon et al., 2012)
KTS022IG	DH10B *ΔptsHIcrr galP^q idnK ΔgntK*	(Solomon et al., 2012)
KTS622IG	DH10B *ΔptsHIcrr galP^q* P_{glk}::J23117[a] *ΔidnK ΔgntK*	(Solomon et al., 2012)
KTS822IG	DH10B *ΔptsHIcrr galP^q* P_{glk}::J23109[a] *ΔidnK ΔgntK*	(Solomon et al., 2012)
KTS922IG	DH10B *ΔptsHIcrr galP^q* P_{glk}::J23114[a] *ΔidnK ΔgntK*	(Solomon et al., 2012)
NVS622IG	DH10B *ΔptsHIcrr galP^q* P_{glk}::(*J61048 tetR B0034* P_{tet} *lacI-LVA J23117 lacO*) *ΔidnKΔgntK*	This study
NVS922IG	DH10B *ΔptsHIcrr galP^q* P_{glk}::(*J61048 tetR B0034* P_{tet} *lacI-LVA J23114 lacO*) *ΔidnK ΔgntK*	This study
Plasmids		
pCP20	*λ* cI857 (ts), *λ pr* Rep^{ts}, *bla*(Amp^R), *cat*(Cm^R), *λ* p_r FLP	CGSC#7629
pTrc99ACm-gdh	ColE1(pBR322) *ori*, *cat* (Cm^R), *lacI*, P_{trc} *gdh*	(Solomon et al., 2012)
pBAD30-gdh	*p15A*, *bla* (Amp^R), *araC*, P_{araB} *gdh*	This study
pKVS45	*p15A*, *bla*(Amp^R), *tetR*, P_{tet}	This study
pKVS45-RXXX	*p15A*, *bla*(Amp^R), *tetR*, P_{tet} *RXXX* (asRNA)	This study
pTKRED	*oriR101*, *repA101^{ts}*, *aadA* (Spec^R), *araC*, P_{lac} λ_γ λ_β λ_{exo}, *lacI*, P_{araB} *I-SceI*	(Kuhlman and Cox, 2010)
pTKIP-neo	ColE1(pBR322) *ori*, *bla*(Amp^R), *neo* (Kan^R)	(Kuhlman and Cox, 2010)
pTKS/CS	*p15A*, *cat* (Cm^R), P_{laclq} *tetA*	(Kuhlman and Cox, 2010)
pTKIP-neo-KI06	ColE1(pBR322) *ori*, *bla*(Amp^R), *neo* (Kan^R), (*J61048 tetR B0034* P_{tet} *lacI-LVA J23117 lacO*)	This study
pTKIP-neo-KI09	ColE1(pBR322) *ori*, *bla*(Amp^R), *neo* (Kan^R), (*J61048 tetR B0034* P_{tet} *lacI-LVA J23114 lacO*)	This study

[a] J231xxx=Anderson library promoter (http://partsregistry.org).

Table 2
Oligonucleotides used.

Name	Sequence 5′→3′
pKVS45 construction	
TetR_F	CTATCTCGAGTTAAGACCCACTTTCACATTTAAGTTG
TetR_R2	CTATCCTAGGGTGCTCAGTATCTCTATCACTGATAGG
pB30_F	CTATCTCGAGGATAAGCTGTCAAACATGAGCAG
pB30_R2	CTATCCTAGGTTTCTCCATACCCGTTTTTTG
Antisense RNA construction	
glk as rev −20	CTATGTCGAC GATATCTTTAGCGGAGCAGTTGAAGA
glk as for 10	CTATGAATTCAATAGGTCTTAGCCTGCGAG
glk as for 500	CTATGAATTCTATTCGGCGCAAAATCAAC
glk as for 756	CTATGAATTCGAGATTGAGCGCCAGATTG
glk as for 953	CTATGAATTCCCTAAGGTCTGGCGTAAATG
Inverter cloning	
TetR5′HindII	CTATAAGCTTTCGACTCTAGTGGATCTGCTA
TetR3′EcoRI	CTATGAATTCTTTCTTTTGGGTATAGCGTC
KTS9lacI5′ KpnI	CTATGGTACC**TGTGGAATTGTGAGCGCTCACAATTCCACAGCTAGCATTGTACCTAGGACTGAGCTAGCCATAAA**CTAAGAAACCATTATTATCATGACATTAAC
KTS6lacI5′ KpnI	CTATGGTACC**TGTGGAATTGTGAGCGCTCACAATTCCACAGCTAGCACAATCCCTAGGACTGAGCTAGCTGTCAA**CTAAGAAACCATTATTATCATGACATTAAC
lacI3′HindIII	CTATAAGCTTTTATTAAGCTACTAAAGCGTAGTTTTCG
Landing pad integration	
Glk_LP2X	*CTATTCCTTATGCCGGGGTCAGATACTTAGTTTGCCCAGCTTGCAAAAAGGCATCGCTGCAATTGGT*TTGGCTTCAGGGATGAG
Glk_LP1Xv2	*CACATCACCGACTAATGCATACTTTGTCATTCTTCAACTGCTCCGCTAAAGTCAAAATAATTCTTT*TACGGCCCCAAGGT

Restriction sites for cloning are underlined. Homologous sequences for recombination are *italicized*. Introduced mutations are bolded (promoter) or bolded and underlined (lacO).

Cm-Gdh, IPTG was added as indicated to both the seed culture and 50 ml flask cultures at inoculation. For experiments involving pBAD30-Gdh, 0.02% L-arabinose was added to the flasks at inoculation. asRNA characterization studies were conducted with asRNA induced at inoculation. In enzyme activity and qPCR studies, 50 ml shake flasks were inoculated to a final OD_{600} of ~0.001. 5 ml samples were taken periodically as indicated. These samples were then pelleted and stored at −20 °C until assayed. For gluconate experiments, shake flasks were inoculated to a final OD_{600} of ~0.005 with M9 medium supplemented with 1.5% (w/v) glucose and monitored for 72 h before samples were taken and clarified by centrifugation. The supernatant was then stored at 4 °C until metabolite analysis via HPLC. As appropriate, the antibiotics ampicillin, kanamycin, chloramphenicol, spectinomycin and tetracycline were used at concentrations of 100, 25, 34, 100, and 10 μg/ml respectively.

2.4. Enzyme assays

All enzyme activity assays were performed on crude lysates generated by sonication of 5 ml frozen cell pellets resuspended in 500 μl of 10 mM Tris–HCl (pH=8.0) at ~8 W in 5 × 5 s pulses on ice. The resulting lysates were clarified by centrifugation before being assayed for either Glk or Gdh activity as described previously (Solomon et al., 2012). In brief, one unit of Glk activity will phosphorylate 1.0 μmole/min of D-glucose at pH 7.5 and room temperature in the presence of 3.33 U/ml glucose-6-phosphate

dehydrogenase, 60 mM Tris–HCl, 20 mM magnesium chloride, 8.0 mM ATP, 12.0 mM glucose and 0.9 mM $NADP^+$. Similarly, one unit of Gdh activity oxidizes 1.0 μmole/min of D-glucose at pH 7.6 at room temperature in 60 mM potassium phosphate buffer and 0.67 mM NAD^+. In both assays, reaction progress is measured at a wavelength of 340 nm. Due to the assay chemistry, Glk activity cannot be measured independently of Gdh activity. Enzyme activities reported are normalized by total protein levels as measured in a modified Bradford Assay (Zor and Selinger, 1996).

2.5. Quantification of mRNA levels

Total RNA was isolated from 5 ml of culture at the indicated times using the illustra RNAspin Mini Isolation Kit (GE Healthcare Bio-Sciences, Piscataway, NJ) with an on-column DNaseI treatment according to the kit protocol. Using the QuantiTect Reverse Transcription Kit (Qiagen, Valencia, CA) according to manufacturer's instructions, 0.5 μg of total RNA was treated to remove trace DNA contamination before cDNA was synthesized with random primers. To quantify *glk* mRNA, synthesized cDNA was amplified with primers *glk_disambigF2* (5′-TGCCGCATTTGAAGATAAAGG) and *glk_disambigR* (5′-GATATAAAAGGAAGGATTTACAGAATGTGA) at 300 nM final concentration. *glk* antisense+sense mRNA were quantified with primers *glk_R100_for* (5′-TTGGTGCCGCCCACAT) and *glk_R100_rev* (5′-GCGGAGCAGTTGAAGAATGAC) at 50 nM final concentration. qPCR reactions were performed with 3 μl of cDNA product in a 25 μl reaction with Brilliant II Sybr Green High ROX QPCR Mix (Agilent Technologies, Santa Clara, CA) and the requisite primers on an ABI 7300 Real Time PCR System instrument (Applied Biosystems, Beverly, MA). Transcript levels were quantified in duplicate with appropriate no-template and no-RT controls and are relative to that of the indicated control sample as determined from a standard curve. Reported levels are the averages of replicate flasks, each measured in duplicate.

2.6. Metabolite analysis

Glucose, gluconate (Gnt), 5-ketogluconate (5KG) and acetate levels were measured by HPLC analysis using an Aminex® HPX-87H anion exchange column (Bio-Rad Laboratories, Hercules, CA) on an Agilent 1100 series HPLC instrument (Santa Clara, CA) as described previously (Solomon et al., 2012).

3. Results

3.1. Inducible antisense RNA as a dynamic glucose valve actuator

As an initial attempt to institute dynamic control of Glk activity, we investigated the potential of antisense RNA (asRNA) as a valve actuator. While relatively uncommon in prokaryotic systems, there has been increasing interest in the use of RNA-based gene expression control systems for biotechnology applications (Biedendieck et al., 2009; Callura et al., 2010, 2012; Desai and Papoutsakis, 1999; Isaacs et al., 2004; Kim et al., 2009; Kim and Cha, 2003; Tummala et al., 2003a, 2003b). The few examples of such natural and engineered systems extant in the literature are diverse in their approach with equally diverse design rules for asRNA constructs stressing the strength of the binding interaction (Lu and Mathews, 2008; Mutalik et al., 2012), kinetics of hybridization (Patzel and Sczakiel, 1998; Wang and Drlica, 2003) or the structure of the construct itself (Patzel and Sczakiel, 1998; Tummala et al., 2003b). Successful designs have been noted to be short (< 100 nts) (Callura et al., 2010, 2012; Good, 2003; Isaacs et al., 2004) or long with significant complementarity to the ORF (Biedendieck et al., 2009; Desai and Papoutsakis, 1999; Kim and Cha, 2003; Tummala et al., 2003a,2003b); with single hairpins (Callura et al., 2012; Good, 2003) or more complex architecture for stability (Patzel and Sczakiel, 1998; Tummala et al., 2003b). Among these conflicting designs, however, is an emerging consensus that the 5′ UTR, in particular the ribosome binding site (RBS), is critical for functional asRNA (Biedendieck et al., 2009; Callura et al., 2012; Desai and Papoutsakis, 1999; Good, 2003; Isaacs et al., 2004; Kim et al., 2009; Kim and Cha, 2003; Tummala et al., 2003b). Adopting a compromise of these conflicting rules previously demonstrated to be successful (Biedendieck et al., 2009; Desai and Papoutsakis, 1999; Kim et al., 2009; Kim and Cha, 2003), we created asRNA constructs by simply inverting a contiguous sequence stretch of the *glk* operon. These constructs began 20 bps upstream of the start codon, encompassing the RBS, and extended into the ORF. To explore issues such as construct length and the effect of asRNA structure on activity, we truncated these constructs to 4 different lengths. All constructs were expressed from a tetracycline inducible vector, pKVS45 (Fig. 1).

Given the correlation between Glk activity and specific growth rate (Solomon et al., 2012), these constructs were first screened for growth in minimal medium supplemented with 1.5% (w/v) glucose. Upon induction, 2 of the constructs displayed noticeable reductions in specific growth rate (> 5%); R100 and R953 were observed to reproducibly inhibit growth by 7% and 10%, respectively, when induced with 100 ng/ml anhydrotetracycline (aTc) (Fig. 2A). These growth differences, however, did not affect final biomass accumulation. These constructs produced decreases in Glk activity of 12% and 25%, respectively (Fig. 2B). Finally, to evaluate the performance of all constructs, a qRT-PCR assay was used to measure the various RNA

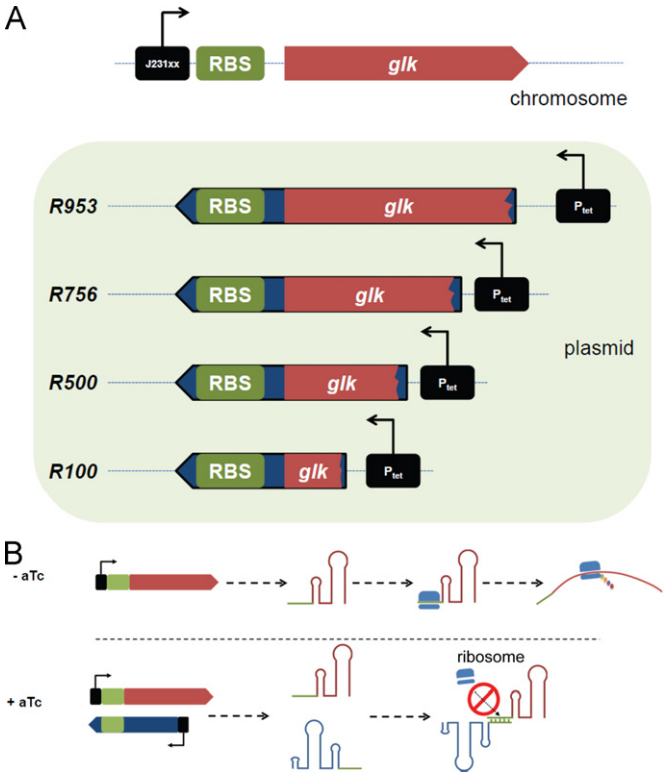

Fig. 1. Antisense glucose valves. (A) Valve schematic. The reverse complement of the RBS and the truncated *glk* ORF are expressed from a plasmid-based inducible Tet promoter. The construct name specifies the number of bases of the ORF incorporated into the antisense RNA. (B) Valve mode of action. In the absence of aTc, *glk* mRNA is transcribed and translated normally into Glk protein. When induced with anhydrotetracyline (aTc), however, antisense RNA, indicated in blue, is transcribed and hybridizes with *glk* mRNA preventing translation (depicted) and/or stimulating mRNA degradation (not depicted).

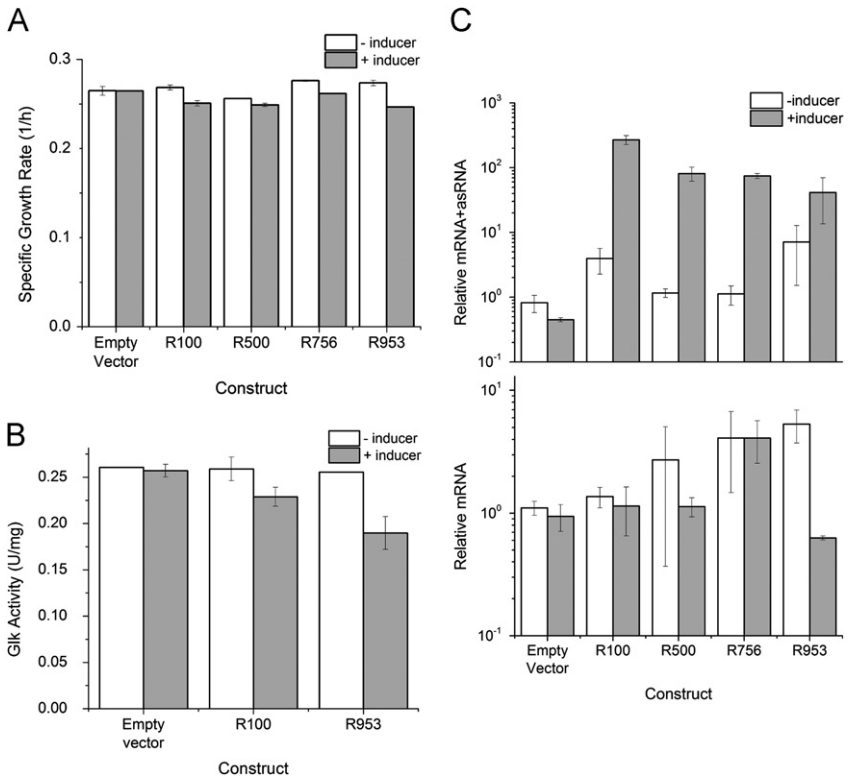

Fig. 2. asRNA characterization. (A) Valve performance as measured by specific growth rate as a function of induction condition. (B) Valve performance as measured by specific Glk activity of the most promising constructs from (A). (C) Valve characterization at the RNA level. RNA levels are relative to a single uninduced empty vector control. Constructs were induced with with 100 ng/ml aTc (indicated with gray bars). All cultures grown in 1.5% glucose supplemented M9 medium. Graphs depict the duplicate mean ± SD of a representative experiment at mid exponential phase (~20–29 h).

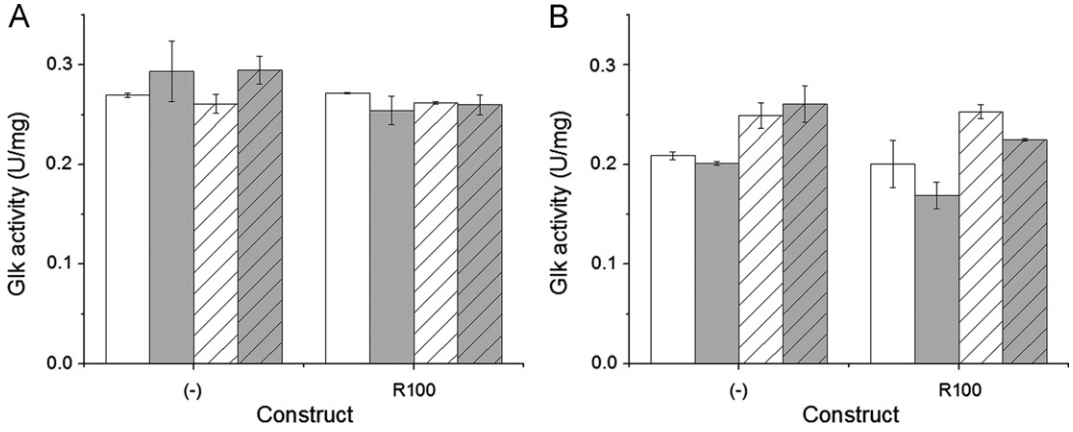

Fig. 3. Effects of medium composition on antisense performance. Performance of an empty vector (pKVS45) and R100 in (A) M9(0.4% glucose) and (B) M9(0.4% glycerol) at 20 h (no fill pattern) and 48 h (hatched bars). Uninduced samples are white and samples induced with 100 ng/ml aTc represented by gray. (–) Control is an empty vector (pKVS45). Figure represents the mean ± SD of duplicate 50 ml flasks of KTS622 at 37 °C.

species. Due to the complementarity between the (sense) mRNA and asRNA, primers to detect asRNA will necessarily measure mRNA levels as well; however, the truncated nature of the asRNA allows selective mRNA amplification of the 3′ end of *glk*. A common primer set for all asRNA constructs was designed by targeting a ~60 bp amplicon near the 5′ terminus of the *glk* CDS while mRNA was amplified with primers targeting the 3′ end. Using these primers, it was observed that the pKVS45 expression system is fairly leaky. However, induction with 100 ng/ml aTc led to at least a 10-fold change in asRNA + mRNA levels for all constructs (Fig. 2C) confirming that the non-functional constructs were expressed. Examining the effects of the asRNA on *glk* mRNA, two very different effects were observed for R100 and R953. R100, shown to have up to a 12% decrease in Glk activity, had no effect on mRNA levels suggesting an RBS occlusion mode of action which reduces translational efficiency. In contrast, R953 was observed to reduce *glk* mRNA by more than 85% and suggests that R953 binding stimulates increased mRNA degradation. Despite this large change in mRNA, however, only a 25% decrease in activity was observed (Fig. 2D). Repeated tests of these constructs under gluconeogenic and glycolytic conditions confirmed the significance and repeatability of this observation (data not shown).

Given the weak correlation between *glk* mRNA and Glk activity in R953, we sought to identify modes of feedback that could potentially explain the discrepancy. In so doing, we noted that the antisense performance was sensitive to medium composition (Fig. 3). In minimal medium supplemented with low levels of glucose (0.4% w/v), the growth trends are consistent with those in

1.5% glucose (Fig. 2A); however, activity differences for the active asRNA constructs are transient and indistinguishable from noise (Fig. 3A). When grown in minimal medium supplemented with glycerol, the activity trends are perceptible and persist with time (Fig. 3B). The literature presented no known genetic mechanisms to explain these observations; however, we realized that the coupling between Glk activity and specific growth rate in glucose, but not glycerol, supplemented medium (Solomon et al., 2012), may offer a potential explanation. Glk, like most bacterial proteins, is fairly stable (Wilkins et al., 1999) and essentially only diluted by growth. This stability passively generates a negative feedback mechanism (Klumpp et al., 2009), which we have termed *growth mediated buffering*, to somewhat regulate carbon flux and Glk activity. For a fixed expression level of *glk*, Glk activity, specific growth rate and carbon flux are in equilibrium. If the system is perturbed with an increase in *glk* expression, Glk activity, carbon flux and specific growth rate increase. This increase in specific growth rate dilutes Glk activity, reducing carbon flux, and buffers the cell against large perturbations. Conversely, lowering *glk* expression would decrease the growth rate and concentrate Glk to minimize the impact on carbon flux. This effect is further convoluted by feedback inhibition of Glk by PEP (Ogawa et al., 2007) and metabolite efficiency or increased enzyme specific activity due to the increased metabolite pool size (Fendt et al., 2010). Based on these facts and the evidence gathered, we propose the following model. In glycerol, Glk activity is decoupled from cell physiology and asRNA trends observed represent their true potential. At high levels of glucose supplementation, carbon flux through the cell is high and the *in vivo* activity of Glk is inhibited below its total activity by PEP. asRNA modulation of Glk leads to reduced carbon flow through glycolysis. This in turn leads to a reduction of PEP repression and increased metabolite efficiency. However, this response is insufficient to counter the gross reduction in flux leading to changes in the observed specific growth rate, growth mediated buffering and the increased noise in Glk total activity. For low levels of glucose supplementation, PEP regulation and metabolite efficiency is minimal due to the reduced carbon flux and thus glycolytic flux changes are much larger than in the high glucose case. This leads to larger growth rate changes and buffering which concentrate Glk to a point where changes in expression are no longer perceptible (Fig. 3A). Thus, we offer that the coupling of growth with Glk activity leads to emergent behavior that regulates carbon flux and Glk activity regardless of *glk* expression levels.

3.2. Effect of asRNA expression on product yields

The ability of these asRNA constructs to redirect carbon towards a competing heterologous pathway was investigated next. The one step conversion of glucose to gluconate described previously was used as a model system (Solomon et al., 2012). Given the sensitivity of gluconate production to cell physiology (Solomon et al., 2012) we first evaluated the ability of the system to tolerate multiple plasmids encoding for our pathway of interest and the asRNA construct itself. As an initial study, pTrc-99 Cm-Gdh, containing glucose dehydrogenase for gluconate production, and the parental pKVS45 plasmid, used to express the asRNA, were tested in four members of a previously constructed glucokinase expression mutant library (Solomon et al., 2012). The presence of the additional plasmid was not necessarily deleterious as trends with induction level generally agreed with those reported previously (Solomon et al., 2012). At an induction level of 25 μM IPTG, production of gluconate from the lowest activity Glk strain (KTS822IG) was observed to increase by at least 300% to titers in excess of 0.5 g/L (Table 3) when compared to a single plasmid context (Solomon et al., 2012). Despite the low glucose consumption, under these conditions, KTS822IG had the highest yield of gluconate. More modest changes were noted for the remaining strains. Evaluating the conversion of glucose into gluconate derived species, we observed a direct monotonic correlation between Glk activity and gluconate molar yield (Fig. 4) confirming the reported observation that Glk may be used to control productivity of a heterologous pathway (Solomon et al., 2012). However, as reported previously, this effect was highly sensitive to parameters such as IPTG induction level (data not shown).

Encouraged by these results, we then tested the ability of asRNA constructs R100 and R953 to inducibly control the productivity of our test pathway. In static tests where the asRNA was induced at inoculation, we were unable to reliably change pathway efficiency. The presence of either asRNA construct occasionally displayed some improved productivity over the empty vector control under various conditions; induction, however, generally provided no further improvement. Similarly, testing the constructs in various hosts of the glucokinase family resulted in inconclusive results. Only in a handful of experiments did induction provide some benefit. The reproducibility and significance of this effect, however, are unclear and may be a product of the transient asRNA response (Fig. 3A). We also considered the possibility of dynamically inducing the asRNA but were unable to see any changes in Glk activity unless the asRNA was induced at inoculation. From this, we concluded that the small nominal dynamic range of the asRNA constructs coupled with the regulatory mechanisms discussed and other phenotypic changes can easily negate their effects, making them unsuitable for future engineering efforts.

3.3. Inverting gene circuit as a dynamic glucose valve activator

Given the results with asRNA, we opted to create a system with parts previously reported to be functional and with a

Table 3
Titers of the major fermentation products as a function of Glk expression. Final OD_{600}, and titers of gluconate (Gnt), its reduced form (5-ketogluconate or 5 KG), acetate and glucose consumed at 72 h. Average values of triplicate cultures are reported with standard deviations given in parentheses. Flasks were grown in M9 (1.5% (w/v) glucose) and induced with 25 μM IPTG. All cultures contain a plasmid for Gdh expression and an empty vector plasmid as surrogate for the antisense valve.

Strain[a]	Final OD_{600}	Estimated[b] Glk activity [U/mg]	Titers			Glucose consumed [g/L]
			Gnt [g/L]	5KG [g/L]	Acetate [g/L]	
KTS822IG	0.24 (0.04)	0.23 (0.04)	0.53 (0.03)	0.03 (0.01)	ND	0.87 (0.27)
KTS622IG	0.98 (0.09)	0.30 (0.02)	3.33 (0.10)	0.17 (0.01)	0.32 (0.14)	7.45 (0.27)
KTS022IG[c]	1.01 (0.08)	0.33 (0.02)	3.32 (0.03)	0.19 (0.01)	0.28 (0.08)	7.05 (0.09)
KTS922IG	1.29 (0.13)	0.50 (0.03)	2.25 (0.40)	0.20 (0.12)	0.82 (0.09)	7.34 (0.25)

ND: not detected.

[a] Mutants spanning roughly 0.5–2 × wildtype growth rates (Solomon et al., 2012).

[b] Due to similar assay chemistries, Glk cannot be measured in the presence of Gdh. Glk activity values reported are of the parental strain in the absence of any plasmid (Solomon et al., 2012).

[c] Native Glk expression.

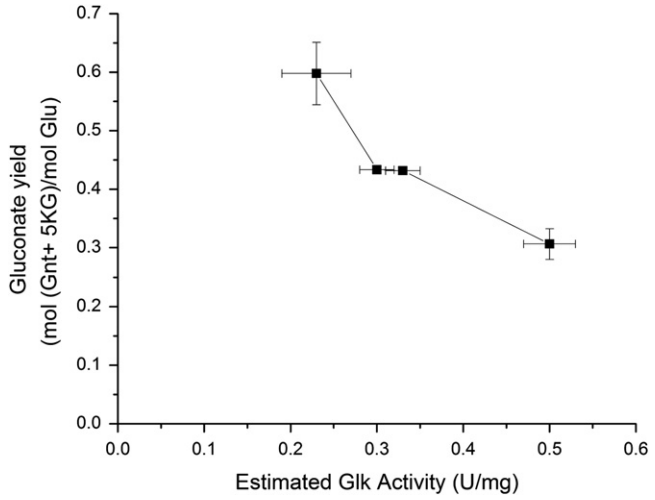

Fig. 4. Relationship between Glk activity and productivity at 72 h. Gluconate molar yield plotted as a function of Glk activity in cells bearing a plasmid for Gdh expression and an empty vector plasmid as surrogate for the antisense valve. Graph depicts the triplicate mean ± SD of a representative experiment. Due to the similar assay chemistries, Glk activity cannot be measured in the presence of Gdh. Estimated Glk activities presented here represent those of the KTSx22IG parent strain (Solomon et al., 2012) in the absence of any plasmid.

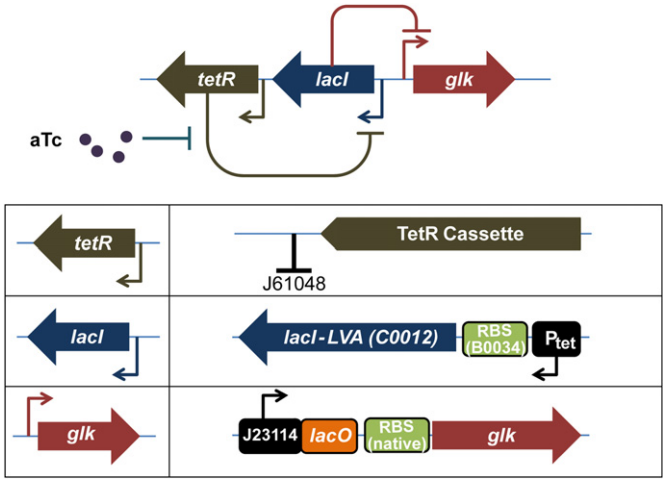

Fig. 5. Inverting glucose valve schematic. Schematic of genetic inverter (NVS922IG) with a detailed description of each module. Alphanumeric codes refer to part numbers within the Registry of Standard Biological Parts (http://partsregistry.org). J61048—transcription terminator; C0012—*lacI* fused with an LVA degradation tag; B0034—a ribosome binding site; J23114—Anderson promoter library variant. TetR cassette refers to the TetR ORF and promoters from pKVS45 while P_{tet} is the inducible Tet promoter also found in pKVS45.

potentially larger dynamic range while still offering a similar inverse transfer curve. Based on these criteria, an inverting gene circuit or inverter was selected. First demonstrated in 2002 (Yokobayashi et al., 2002), an inverter is a basic gene circuit analogous to a NOT logic gate. In our design, TetR is constitutively expressed and regulates expression of *lacI*. LacI, in turn, controls expression of *glk*. In response to aTc supplementation, TetR is repressed driving expression of *lacI* which turns OFF *glk* expression (Fig. 5).

We constructed the inverter by harvesting the TetR expression cassette from pKVS45 and using its Tet promoter to drive expression of LacI modified with an LVA-degradation tag. The *lacI* and *tetR* cassettes were oriented opposite to *glk* to preclude read-through transcription. The LVA-degradation tagged variant of LacI from the Registry of Standard Biological Parts (http://partsregistry.org) was selected to reduce steady state levels of LacI in the system and minimize the deleterious effects of leaky *lacI* expression in the ON configuration. Similarly, no transcriptional terminators were placed between *lacI* and *tetR* to provide negative feedback for leaky *lacI* expression. To create a LacI sensitive promoter, a previously used constitutive promoter from the Anderson Collection in the Registry was fused to a symmetric *lacO* operator (Sadler et al., 1983) directly downstream. The circuit was insulated from the genome with a transcriptional terminator from the Registry placed downstream of *tetR*. The resulting construct was then integrated into the genome directly upstream of *glk*, replacing the FruR binding site through the primary native promoter (P1) (Mendoza-Vargas et al., 2009; Meyer et al., 1997) (Fig. 5).

Two main variants of the inverter were created: NVS922IG and NVS622IG. NVS922IG was constructed with J23114 (http://partsregistry.org), a promoter corresponding to roughly twice the native *glk* promoter strength (Solomon et al., 2012). Similarly, NVS622IG was designed with J23117 (http://partsregistry.org), a promoter approximately equivalent to the native *glk* promoter in strength (Solomon et al., 2012). NVS622IG, however, ultimately proved non-viable in minimal medium supplemented with glucose. NVS922IG was initially characterized by supplementing cultures with either IPTG and/or aTc at inoculation and measuring the Glk activity 20 h later in mid-exponential phase (Fig. 6). aTc was seen to suppress Glk activity, demonstrating a successful inversion response. Moreover, IPTG and aTc supplementation were able to recover Glk activity, confirming the mechanism of action. IPTG induction alone, however, could increase the ON state expression of Glk by ~40% (Fig. 6). This indicates significant leaky *lacI* expression is present which may be sufficient to suppress *glk* expression in the ON state to such a degree that NVS622IG is unable to attain the Glk levels necessary to sustain growth.

NVS922IG was characterized more thoroughly by growing cells in minimal medium supplemented with 0.4% (w/v) glycerol and inducing with aTc at one of 6 levels at inoculation. After 27 h the cells were at approximately steady state (mid-late exponential phase, OD_{600} ~0.5–0.9), with the exception of the highest induction level (OD_{600} ~0.1). At this time samples were taken and assayed for Glk activity and *glk* mRNA abundance. The ON, or uninduced state, had an activity of 0.29 ± 0.01 U/mg, which was significantly lower than the system using the same promoter in isolation (0.42 U/mg ± 0.02 U/mg—(Solomon et al., 2012)) and is likely attributable to leaky *lacI* expression as described above. The inverter, nonetheless, was observed to control Glk activity in a dose-dependent manner with a canonical sigmoidal relationship. Full suppression of Glk was achieved at approximately 100 ng/ml aTc (Fig. 7). Evaluating the *glk* mRNA abundance relative to the uninduced state, a similar dose-dependent sigmoidal relationship with up to 80% repression in mRNA levels was observed (Fig. 7).

Dynamic control with NVS922IG and its performance under more relevant glycolytic growth conditions were evaluated in triplicate flasks containing minimal medium supplemented with 1.5% (w/v) glucose. At early-exponential phase (OD~0.25) each flask was split into two equal volumes with a flask from each pair induced with 100 ng/ml aTc (Fig. 8A). The OD_{600}, Glk activity and *glk* mRNA of these flasks were tracked over time. As a control, another flask was grown and induced at inoculation. Uninduced flasks had specific growth rates and activities comparable to native levels in glucose supplemented medium (μ~0.3 1/h; activity~0.23 U/mg; Solomon et al., 2012). As anticipated, the induced control failed to grow due to low *glk* expression. In the induced split flasks, however, there is an immediate divergence in specific growth rate from the uninduced flasks, with growth persisting for at least 30 h post induction (Fig. 8B). As noted in our previous report (Solomon et al., 2012), control of Glk in this

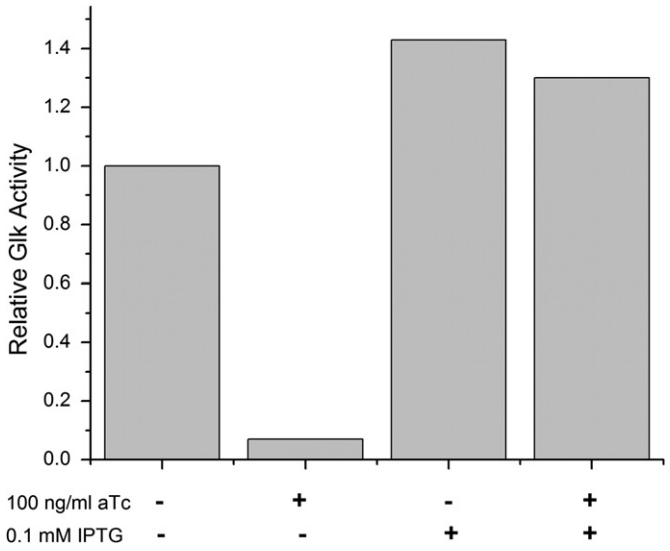

Fig. 6. Initial characterization of a genetic inverter. Glk activity of NVS922IG as a function of aTc and IPTG induction level at 20 h in 0.4% (w/v) glycerol supplemented minimal medium. Activity is relative to the uninduced control.

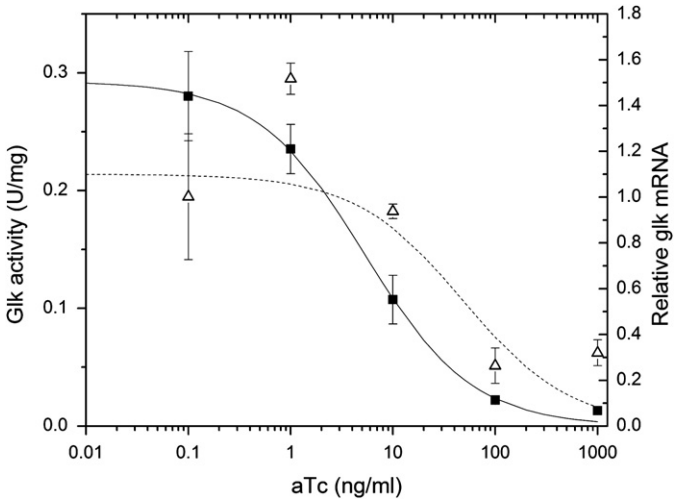

Fig. 7. Genetic inverter performance. Performance of NVS922IG at the protein (filled squares) and RNA (open triangle) levels as a function of aTc in 0.4% (w/v) glycerol supplemented minimal medium at 27 h. RNA levels are relative to an uninduced control. Unbroken and dashed lines represent a best fit to a Hill function of the activity and mRNA data, correspondingly. Uninduced specific activity and relative mRNA are 0.29 ± 0.01 U/mg and 1.06 ± 0.08, respectively. Graph depicts the triplicate mean $\pm$ SD.

manner offers true dynamic control of glucose flux and macroscopic behavior such as specific growth rate, unlike control at nodes further downstream in glycolysis (Cho et al., 2012). Evaluating the relative changes of the induced to uninduced flasks across the macroscopic, protein and RNA levels, a consistent steady state decrease of $\sim$50% is seen (Fig. 8C). Despite the uniformity of performance across levels, however, the dynamic performance of the inverter at the protein level is inconsistent with the behavior noted in glycerol supplemented medium (Fig. 7) or even glucose supplemented medium when it is induced at inoculation (Fig. 8B). Given these earlier studies, it was anticipated that induction of the inverter would fully arrest growth. However, this inconsistency may be understood in light of the growth mediated buffering presented earlier: the reduced specific growth rate that accompanies inverter induction concentrates Glk to a level that allows growth to persist.

Changes are noticeably faster at the protein level, with the system reaching steady state within 5 h, before being propagated to the macroscopic level ($t_{\text{steady state}} > 20$ h). The response time at the protein level is consistent with theoretical predictions. With transcription rates and mRNA lifetimes typically on the order of minutes (Bremer and Dennis, 2008; Vogel and Jensen, 1994), translation rates of *lacI* on the order of minutes (Bremer and Dennis, 2008) and no active degradation of Glk, the dynamics of Glk levels are anticipated to be controlled by dilution due to growth. Indeed, analyzing the dynamic protein data an exponential decay time constant of 3.74 ± 1.91 h was obtained which yields a protein half-life (2.59 ± 1.33 h) approaching the doubling time of uninduced cells (2.23 h).

3.4. Effect of inverter expression on product yields

Finally, we evaluated the potential of our system to redirect carbon into gluconate production. As the inverter is IPTG responsive (Fig. 6), pBAD30 (Guzman et al., 1995) rather than pTrc99Cm was used to express Gdh. Due to the *ptsHIcrr galP*^{q} background of the inverter host, catabolite repression of arabinose induction in the presence of glucose is no longer active (Hernandez-Montalvo et al., 2001). NVS922IG was inoculated in triplicate in M9 medium supplemented with glucose and Gdh induced with L-arabinose at inoculation. Cells were grown for at least 19 h into early exponential phase before the inverter was triggered with 100 ng/ml aTc. Titers of major fermentation products and glucose were assayed at 72 h. Inducing the inverter at an $OD_{600} \sim 0.3$, there was a 30% improvement in gluconate titers from 6.14 g/l to 8.04 g/l, a 40% reduction in acetate titers from 0.41 g/l to 0.24 g/l and a slight increase in glucose consumption from 7.3 g/l to 8.2 g/L with negligible change in biomass accumulation relative to uninduced controls (Fig. 9A). Normalizing by glucose consumption on a molar basis, this translates to an 18% improvement in gluconate molar yield (0.70 mol/mol Glu to 0.83 mol/mol Glu) and a 46% reduction in carbon wastage to acetate (0.14 mol/mol Glu to 0.08 mol/mol Glu) (Fig. 9B). This improvement was a strong function of OD_{600} at induction (Fig. 9C). The effect on both gluconate and acetate yields diminished as induction OD_{600} increased and was non-existent for $OD_{600} \geq 1.0$. Such behavior is consistent with Glk degradation being primarily controlled by dilution due to growth. At early OD_{600}, cells have sufficient generations to wash out Glk when the inverter is switched to the OFF state, allowing for the redirection of carbon and yield improvements of the model pathway. As the number of doublings until stationary phase decreases, delayed induction of the inverter decreases its dynamic range resulting in reduced carbon redirection and smaller observed improvements. Different behavior may potentially be observed in a system with destabilized Glk. However, care must be taken in the design of these systems as protein degradation is energy dependent and may introduce unforeseen effects when coupled with reduced carbon flux.

The expression of Gdh as a function of inverter induction level and timing (OD_{600}) was also evaluated. At early times ($\sim$24 h), there was no change in the amount of Gdh measured. However, for a number of cases at 72 h, the induced inverter had a noticeable increase in Gdh activity ($\leq 50\%$), presumably a consequence of the reduced dilution due to growth. Nonetheless, for the earliest OD_{600} at which the inverter was induced ($\sim$0.1), where this effect is likely to be greatest, there was no observed increase in Gdh expression (Fig. 10) suggesting more complex mechanisms governing expression levels. Moreover, there were still improvements in gluconate and acetate yields (Fig. 9C) suggesting that the effects observed are not strongly influenced by Gdh expression. That is, the improvements observed are due in part to carbon flux redirection as designed.

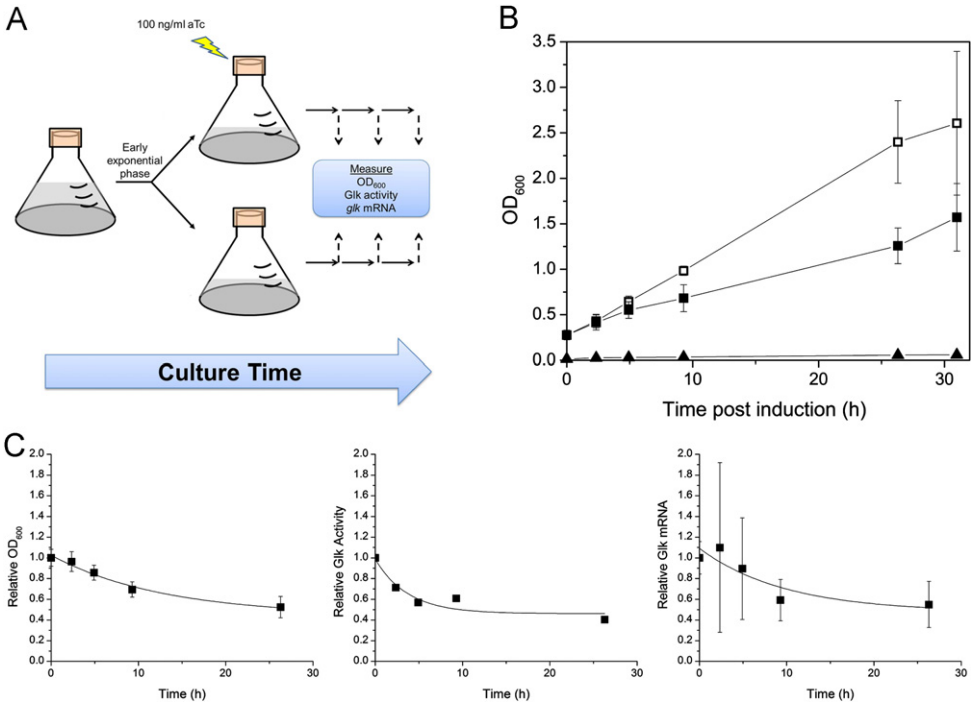

Fig. 8. Dynamic performance of inverter as a glucose valve. (A) Experimental scheme. (B) Optical density (OD_{600}) of split flasks post induction (open squares—uninduced, filled squares—induced) and a representative control culture induced at inoculation (filled triangles). (C) Relative performance of induced:uninduced across macroscopic (growth), protein and mRNA levels. The graph in B depicts the triplicate mean ± SD with the exception of the representative control. The graphs in C represent the triplicate mean ± SEM. Cultures were induced with 100 ng/ml aTc.

4. Discussion

The optimization of metabolic phenotypes frequently requires the rerouting of metabolite flux towards the pathway of interest. While heavily implemented for the engineered production of many primary and secondary metabolites, the controlled diversion of glucose from central carbon metabolism has until recently been relatively unexplored. Of late, groups have begun to explore the effects of flux redirection through glycolytic nodes such as glyceraldehyde-3-phosphate (Cho et al., 2012), glucose 6-phosphate and 6-phosphogluconolactone (Callura et al., 2012). However, none has sought to address the feasibility of using glucose itself as a substrate or its impact on cell physiology. In this work and its companion study (Solomon et al., 2012), we have demonstrated the ability to control glucose distribution through the modulation of Glk and evaluated its impact on cell health.

In order to redirect glucose flux, *E. coli* was reengineered to generate a control node through Glk. This modification made Glk essential for cell growth. Moreover, the direct changes in carbon flux through Glk could alter the phenotype of the cell. However, unlike similar studies where cellular phenotype was directly controlled, only specific growth rates and not biomass accumulation are affected (Cho et al., 2012; Min et al., 2012). These growth rate changes, nonetheless, are accompanied by global changes in protein expression (Klumpp et al., 2009; Scott et al., 2010) and metabolite pools which form negative feedback mechanisms to counter the induced changes (Fendt et al., 2010; Klumpp et al., 2009). The control of central carbon flux also reduces the resources available for the cell to support heterologous expression (Heyland et al., 2011).

We thus pursued a dynamic control strategy to mitigate these negative consequences by reducing the culture time over which they operate. Initially, inducible asRNA was explored. asRNA constructs were developed by inverting the ORF of the target gene and truncating to various lengths. Limited success was achieved with these constructs. Glk activity was inhibited by up to 25%; however, these changes were transient (Fig. 3A) and did not translate into controllable gains in pathway productivity. One potential hypothesis to explain this is the intrinsic negative feedback regulatory mechanism between Glk activity and growth (Klumpp et al., 2009; Solomon et al., 2012) which we have called *growth mediated buffering*: inhibition of Glk activity reduces the specific growth rate and concentrates the remaining Glk, countering the asRNA effects.

To mitigate this effect, we sought larger changes in Glk activity by utilizing well characterized components isolated for synthetic biology applications. In the past, synthetic biology has provided a number of parts, devices and technologies demonstrated to assist the optimization of metabolic production pathways (Agapakis et al., 2010; Dueber et al., 2009; Moon et al., 2010; Pfleger et al., 2006; Wang et al., 2009). Leveraging the 'parts' and crowd-sourced notes curated in the Registry of Standard Biological Parts, we rapidly designed and prototyped a functional inverter. This design was able to reproducibly inhibit growth by up to 50% in a dynamic fashion with up to a 20% increase in pathway efficiency and almost 50% reduction in carbon wasting to acetate. These process gains were not accompanied by limited recombinant protein expression or reduced biomass accumulation as seen in the static control cases despite similar reductions in Glk activity from wildtype (Solomon et al., 2012). Moreover, this implementation of an inverter as a metabolite valve represents a novel application of the growing synthetic biology toolbox. Yield improvements with this valve, however, were maximal when triggered early in growth. This result is likely attributed to the intrinsic stability of Glk; once the inverter is triggered, existing protein may only be removed by dilution due to growth before carbon is effectively redirected. Attempts to destabilize inverter regulated Glk were unsuccessful. The presence of the weak ASV protein degradation tag (Andersen et al., 1998) along with leaky *lacI* expression (Fig. 6) resulted in insufficient Glk to support

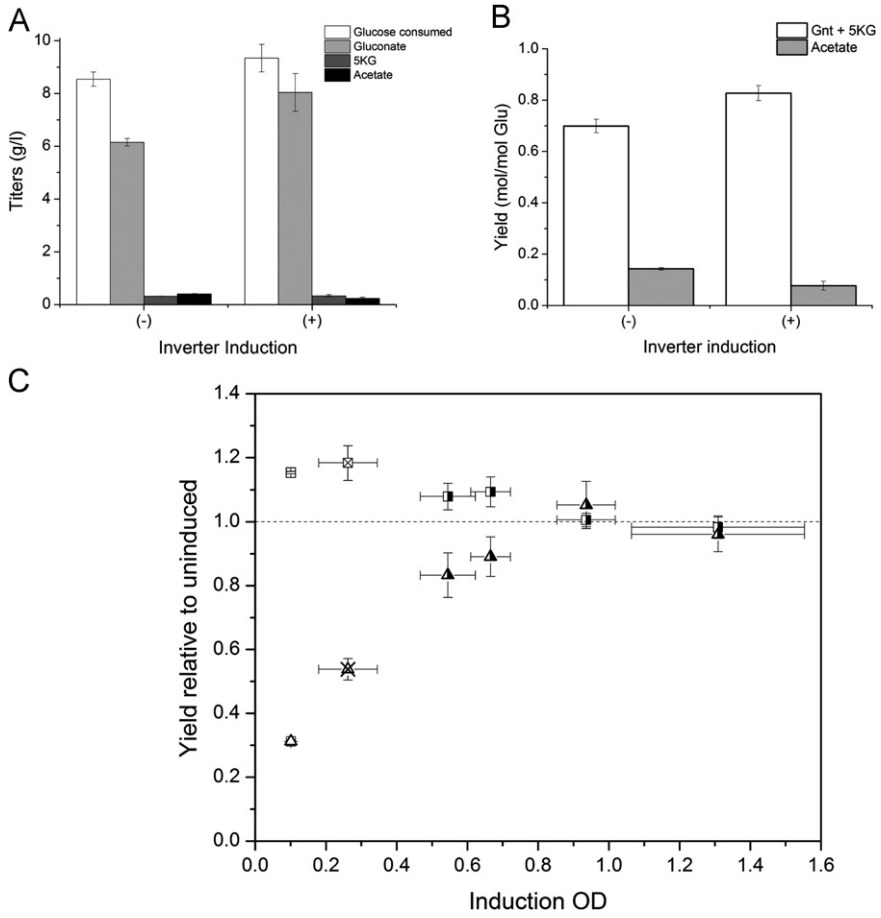

Fig. 9. Effect of inverter on gluconate yield. (A) Titers of major fermentation products. (B) Molar yields of gluconate and acetate of a representative experiment at 72 h for an uninduced control and inverter induced at early exponential phase (OD∼0.3). (C) Molar yield of acetate (triangles) and gluconate (squares) at 72 h of induced inverter relative to an uninduced control as a function of OD at induction. Data from independent experiments are distinguished by fill pattern. In all figures, Gdh was expressed with 0.02% (w/v) L-Ara. The inverter was induced with 100 ng/ml aTc. Data represent the triplicate mean ± SD.

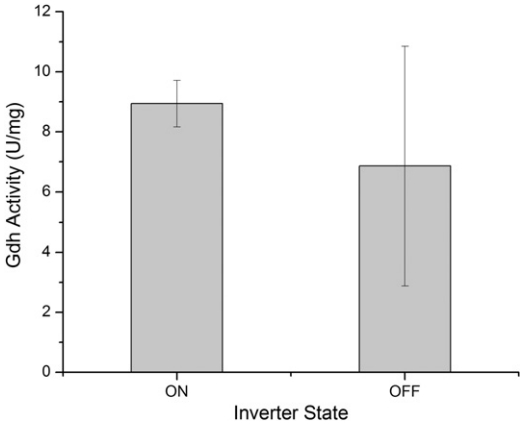

Fig. 10. Gdh activity as a function of Inverter state. Gdh activity of inverter at 72 h when uninduced (ON) and induced with 100 ng/ml aTc at OD_{600}∼0.1 (OFF). Data represents the triplicate mean ± SD of the cultures depicted in Fig. 9C (no fill).

growth. This could potentially be alleviated by redesigning the inverter with a stronger promoter to drive Glk expression. However, expression levels must be carefully tuned so that the additional protein does not swamp either the proteolytic or translational machinery, or exhaust native ATP supplies resulting in cellular death (Solomon et al., 2012).

In this work, we proposed and demonstrated a *glucose valve* to dynamically redirect glucose flux towards heterologous pathways. This paradigm, while relatively new to metabolic engineering, is generalizable to a number of metabolites (Callura et al., 2012; Cho et al., 2012; Farmer and Liao, 2000; Yamanishi and Matsuyama, 2012) with predicted and demonstrated improvements in pathway performance (Anesiadis et al., 2008; Farmer and Liao, 2000). Here, we have successfully engineered controllable redirection of glucose away from central carbon metabolism in a dynamic fashion which, to the best of our knowledge, is one of the first examples reported. In this manner, we were not only able to demonstrate the potential to improve yield and productivity of a heterologous pathway with a dynamic *valve*, but also the ability to reduce carbon waste to acetate and potentially alleviate the demands of pH control in bioprocessing due to acetate accumulation. Furthermore, the redirection of glucose away from central metabolism, especially in a dynamic fashion, enables the generation of new classes of efficient pathways where glucose may be used directly as a substrate.

References

Agapakis, C.M., Ducat, D.C., Boyle, P.M., Wintermute, E.H., Way, J.C., Silver, P.A., 2010. Insulation of a synthetic hydrogen metabolism circuit in bacteria. J. Biol. Eng. 4, 3.

Andersen, J.B., Sternberg, C., Poulsen, L.K., Bjorn, S.P., Givskov, M., Molin, S., 1998. New unstable variants of green fluorescent protein for studies of transient gene expression in bacteria. Appl. Environ. Microbiol. 64, 2240–2246.
Anesiadis, N., Cluett, W.R., Mahadevan, R., 2008. Dynamic metabolic engineering for increasing bioprocess productivity. Metab. Eng. 10, 255–266.
Asadollahi, M.A., Maury, J., Møller, K., Nielsen, K.F., Schalk, M., Clark, A., Nielsen, J., 2008. Production of plant sesquiterpenes in *Saccharomyces cerevisiae*: effect of ERG9 repression on sesquiterpene biosynthesis. Biotechnol. Bioeng. 99, 666–677.
Asadollahi, M.A., Maury, J., Schalk, M., Clark, A., Nielsen, J., 2010. Enhancement of farnesyl diphosphate pool as direct precursor of sesquiterpenes through metabolic engineering of the mevalonate pathway in *Saccharomyces cerevisiae*. Biotechnol. Bioeng. 106, 86–96.
Becker, J., Buschke, N., Bücker, R., Wittmann, C., 2010. Systems level engineering of *Corynebacterium glutamicum*—reprogramming translational efficiency for superior production. Eng. Life Sci. 10, 430–438.
Becker, J., Klopprogge, C., Schroder, H., Wittmann, C., 2009. TCA cycle engineering for improved lysine production in *Corynebacterium glutamicum*. Appl. Environ. Microbiol. 75, 7866–7869.
Biedendieck, R., Malten, M., Barg, H., Bunk, B., Martens, J.-H., Deery, E., Leech, H., Warren, M.J., Jahn, D., 2009. Metabolic engineering of cobalamin (vitamin B12) production in *Bacillus megaterium*. Microb. Biotechnol. 3, 24–37.
Bremer, H., Dennis, P.P., 2008. Modulation of chemical composition and other parameters of the cell at different exponential growth rates. In: Böck, A., C I, R., Kaper, J.B., Karp, P.D., Neidhardt, F.C., Nyström, T., Slauch, J.M., Squires, C.L., Ussery, D. (Eds.), EcoSal—*Escherichia coli* and *Salmonella*: Cellular and Molecular Biology. ASM Press, Washington, DC.
Callura, J.M., Dwyer, D.J., Isaacs, F.J., Cantor, C.R., Collins, J.J., 2010. Tracking, tuning, and terminating microbial physiology using synthetic riboregulators. Proc. Natl. Acad. Sci. USA 107, 15898–15903.
Callura, J.M., Cantor, C.R., Collins, J.J., 2012. Genetic switchboard for synthetic biology applications. Proc. Natl. Acad. Sci. USA 109, 5850–5855.
Cho, H.-S., Seo, S.W., Kim, Y.M., Jung, G.Y., Park, J.M., 2012. Engineering glyceraldehyde-3-phosphate dehydrogenase for switching control of glycolysis in *Escherichia coli*. Biotechnol. Bioeng. , http://dx.doi.org/10.1002/bit.24532.
Curran, K.A., Alper, H.S., 2012. Expanding the chemical palate of cells by combining systems biology and metabolic engineering. Metab. Eng. 14, 289–297.
Datsenko, K.A., Wanner, B.L., 2000. One-step inactivation of chromosomal genes in *Escherichia coli* K-12 using PCR products. Proc. Natl. Acad. Sci. USA 97, 6640–6645.
Demain, A.L., 2000. Microbial biotechnology. Trends Biotechnol. 18, 26–31.
Desai, R.P., Papoutsakis, E.T., 1999. Antisense RNA strategies for metabolic engineering of *Clostridium acetobutylicum*. Appl. Environ. Microbiol. 65, 936–945.
Drew, S.W., Demain, A.L., 1977. Effect of primary metabolites on secondary metabolism. Ann. Rev. Microbiol. 31, 343–356.
Dueber, J.E., Wu, G.C., Malmirchegini, G.R., Moon, T.S., Petzold, C.J., Ullal, A.V., Prather, K.L.J., Keasling, J.D., 2009. Synthetic protein scaffolds provide modular control over metabolic flux. Nat Biotechnol. 27, 753–759.
Farmer, W.R., Liao, J.C., 2000. Improving lycopene production in *Escherichia coli* by engineering metabolic control. Nat. Biotechnol. 18, 533–537.
Fendt, S.-M., Buescher, J.M., Rudroff, F., Picotti, P., Zamboni, N., Sauer, U., 2010. Tradeoff between enzyme and metabolite efficiency maintains metabolic homeostasis upon perturbations in enzyme capacity. Mol. Syst. Biol., 6.
Good, L., 2003. Translation repression by antisense sequences. Cell. Mol. Life Sci. 60, 854–861.
Guzman, L.M., Belin, D., Carson, M.J., Beckwith, J., 1995. Tight regulation, modulation, and high-level expression by vectors containing the arabinose PBAD promoter. J. Bacteriol. 177, 4121–4130.
Hernandez-Montalvo, V., Valle, F., Bolivar, F., Gosset, G., 2001. Characterization of sugar mixtures utilization by an *Escherichia coli* mutant devoid of the phosphotransferase system. Appl. Microbiol. Biotechnol. 57, 186–191.
Heyland, J., Blank, L.M., Schmid, A., 2011. Quantification of metabolic limitations during recombinant protein production in *Escherichia coli*. J. Biotechnol. 155, 178–184.
Isaacs, F.J., Dwyer, D.J., Ding, C.M., Pervouchine, D.D., Cantor, C.R., Collins, J.J., 2004. Engineered riboregulators enable post-transcriptional control of gene expression. Nat. Biotechnol. 22, 841–847.
Kim, J., Hirasawa, T., Sato, Y., Nagahisa, K., Furusawa, C., Shimizu, H., 2009. Effect of odhA overexpression and odhA antisense RNA expression on Tween-40-triggered glutamate production by *Corynebacterium glutamicum*. Appl. Microb. Biotechnol. 81, 1097–1106.
Kim, J.Y.H., Cha, H.J., 2003. Down-regulation of acetate pathway through antisense strategy in *Escherichia coli*: improved foreign protein production. Biotechnol. Bioeng. 83, 841–853.
Klumpp, S., Zhang, Z., Hwa, T., 2009. Growth rate-dependent global effects on gene expression in bacteria. Cell 139, 1366–1375.
Kuhlman, T.E., Cox, E.C., 2010. Site-specific chromosomal integration of large synthetic constructs. Nucleic Acids Res. 38, e92.
Lim, D.B., Oppenheim, J.D., Eckhardt, T., Maas, W.K., 1987. Nucleotide sequence of the argR gene of *Escherichia coli* K-12 and isolation of its product, the arginine repressor. Proc. Natl. Acad. Sci. USA 84, 6697–6701.
Lu, Z.J., Mathews, D.H., 2008. OligoWalk: an online siRNA design tool utilizing hybridization thermodynamics. Nucleic Acids Res. 36, W104–W108.
Mendoza-Vargas, A., Olvera, L., Olvera, M., Grande, R., Vega-Alvarado, L., Taboada, B., Jimenez-Jacinto, V., Salgado, H., Juarez, K., Contreras-Moreira, B., Huerta, A.M., Collado-Vides, J., Morett, E., 2009. Genome-wide identification of transcription start sites, promoters and transcription factor binding sites in *E. coli*. PLoS One 4, e7526.
Meyer, D., Schneider-Fresenius, C., Horlacher, R., Peist, R., Boos, W., 1997. Molecular characterization of glucokinase from *Escherichia coli* K-12. J. Bacteriol. 179, 1298–1306.
Min, B.E., Seo, S.W., Jung, G.Y., 2012. Switching control of an essential gene for reprogramming of cellular phenotypes in *Escherichia coli*. Biotechnol. Bioeng. 109, 1875–1880.
Moon, T.S., Dueber, J.E., Shiue, E., Prather, K.L.J., 2010. Use of modular, synthetic scaffolds for improved production of glucaric acid in engineered *E. coli*. Metab. Eng. 12, 298–305.
Mutalik, V.K., Qi, L., Guimaraes, J.C., Lucks, J.B., Arkin, A.P., 2012. Rationally designed families of orthogonal RNA regulators of translation. Nat. Chem. Biol. 8, 447–454.
Ogawa, T., Mori, H., Tomita, M., Yoshino, M., 2007. Inhibitory effect of phosphoenolpyruvate on glycolytic enzymes in *Escherichia coli*. Res. Microbiol. 158, 159–163.
Patzel, V., Sczakiel, G., 1998. Theoretical design of antisense RNA structures substantially improves annealing kinetics and efficacy in human cells. Nat. Biotechnol. 16, 64–68.
Pfleger, B.F., Pitera, D.J., Smolke, C.D., Keasling, J.D., 2006. Combinatorial engineering of intergenic regions in operons tunes expression of multiple genes. Nat. Biotechnol. 24, 1027–1032.
Sadler, J.R., Sasmor, H., Betz, J.L., 1983. A perfectly symmetric lac operator binds the lac repressor very tightly. Proc. Natl. Acad. Sci. USA 80, 6785–6789.
Sambrook, J., Russell, D.W., 2001. Molecular Cloning: A Laboratory Manual. Cold Spring Harbor Laboratory Press, Cold Spring Harbor.
Scott, M., Gunderson, C.W., Mateescu, E.M., Zhang, Z., Hwa, T., 2010. Interdependence of cell growth and gene expression: origins and consequences. Science 330, 1099–1102.
Shimizu, Y., Shimizu, N., Hayashi, M., 1973. In vitro repression of transcription of the tryptophan operon by trp repressor. Proc. Natl. Acad. Sci. USA 70, 1990–1994.
Shoeman, R., Redfield, B., Coleman, T., Greene, R.C., Smith, A.A., Brot, N., Weissbach, H., 1985. Regulation of methionine synthesis in *Escherichia coli*: effect of metJ gene product and S-adenosylmethionine on the expression of the metF gene. Proc. Natl. Acad. Sci. USA 82, 3601–3605.
Solomon, K.V., Moon, T.S., Ma, B., Sanders, T.M., Prather, K.L.J., 2012. Tuning primary metabolism for heterologous pathway productivity. ACS Synth. Biol. , http://dx.doi.org/10.1021/sb300055e.
Stojiljkovic, I., Baumler, A.J., Hantke, K., 1994. Fur regulon in gram-negative bacteria. Identification and characterization of new iron-regulated *Escherichia coli* genes by a fur titration assay. J. Mol. Biol. 236, 531–545.
Tabor, J.J., Salis, H.M., Simpson, Z.B., Chevalier, A.A., Levskaya, A., Marcotte, E.M., Voigt, C.A., Ellington, A.D., 2009. A synthetic genetic edge detection program. Cell 137, 1272–1281.
Tummala, S.B., Junne, S.G., Papoutsakis, E.T., 2003a. Antisense RNA downregulation of coenzyme A transferase combined with alcohol-aldehyde dehydrogenase overexpression leads to predominantly alcohologenic *Clostridium acetobutylicum* fermentations. J. Bacteriol. 185, 3644–3653.
Tummala, S.B., Welker, N.E., Papoutsakis, E.T., 2003b. Design of antisense RNA constructs for downregulation of the acetone formation pathway of *Clostridium acetobutylicum*. J. Bacteriol. 185, 1923–1934.
Vogel, U., Jensen, K.F., 1994. The RNA chain elongation rate in *Escherichia coli* depends on the growth rate. J. Bacteriol. 176, 2807–2813.
Wang, H.H., Isaacs, F.J., Carr, P.A., Sun, Z.Z., Xu, G., Forest, C.R., Church, G.M., 2009. Programming cells by multiplex genome engineering and accelerated evolution. Nature 460, 894–898.
Wang, J.Y., Drlica, K., 2003. Modeling hybridization kinetics. Math. Biosci. 183, 37–47.
Wilkins, M.R., Gasteiger, E., Bairoch, A., Sanchez, J.C., Williams, K.L., Appel, R.D., Hochstrasser, D.F., 1999. Protein identification and analysis tools in the ExPASy server. Methods Mol. Biol. 112, 531–552.
Yamanishi, M., Matsuyama, T., 2012. A modified cre-lox genetic switch to dynamically control metabolic flow in *Saccharomyces cerevisiae*. ACS Synth. Biol. 1, 172–180.
Yokobayashi, Y., Weiss, R., Arnold, F.H., 2002. Directed evolution of a genetic circuit. Proc. Natl. Acad. Sci. USA 99, 16587–16591.
Zor, T., Selinger, Z., 1996. Linearization of the Bradford protein assay increases its sensitivity: theoretical and experimental studies. Anal. Biochem. 236, 302–308.